http://dx.doi.org/10.5935/0103-5053.20150228

J. Braz. Chem. Soc., Vol. 27, No. 2, 285-294, 2016.
Printed in Brazil - ©2016 Sociedade Brasileira de Química
0103 - 5053 $6.00+0.00

Article

Multifunctional Imidazole-Derived Polymeric Catalyst for Dephosphorylation Reactions Potentiated by Cationic and Anionic Micelles

***Elisa S. Orth*[*,a] and Renan B. Campos*[#,b]**

[a]*Departmento de Química, Universidade Federal do Paraná (UFPR), CP 19081, 81531-990 Curitiba-PR, Brazil*

[b]*Departamento de Química e Biologia, (DAQBi), Universidade Tecnológica Federal do Paraná (UTFPR), 80230-901 Curitiba-PR, Brazil*

Results confirm the catalytic potential of imidazole groups anchored on the polymeric backbone of polyvinylimidazole (PVI) in dephosphorylation reactions with di- and tri-phosphoesters, promoting impressive enhancements up to 10^7-fold. We propose the imidazole groups on PVI react by nucleophilic catalysis (neutral specie) with a phosphate triester and bifunctionally by general acid-nucleophilic catalysis (bipolar species) with a diester. Additionally, PVI can incorporate the reactants on its domains by hydrophobic and electrostatic attraction, confirming the polymer multifunctionality. Moreover, a pronounced micellar catalysis was observed for the reactions which, surprisingly, occurs with both cationic and anionic micelles, due to favorable approximation effects. The micellar effects observed confirms the reactivity of the bipolar species. Based on the pseudophase model, the reagents can be incorporated in the micellar phase, mainly by hydrophobic forces. Overall, we confirm that PVI has great potential as an artificial enzyme, since it undergoes enzymatic-like mechanisms with an elegant bifunctional catalysis.

Keywords: micellar catalysis, dephosphorylation, imidazole, polymeric catalysis

Introduction

Dephosphorylation reactions govern many biological functions[1] and there is an increasing interest in mimicking these reactions with catalysts inspired on the highly efficient natural enzymes, due to their intriguing multifunctional nature. Particularly, the imidazole (IMZ) group has outlined many successful studies,[2] since is present in innumerous enzymatic active sites as histidine residue.[3-6] We have reported some IMZ-based inter- and intra-molecular models,[7-11] shown in Scheme 1 with impressive rate enhancements, arising from nucleophilic and/or general-acid catalysis.

Our results presented so far, for dephosphorylation reactions in the presence of the IMZ group, allowed a comprehensive understanding of the mechanistic

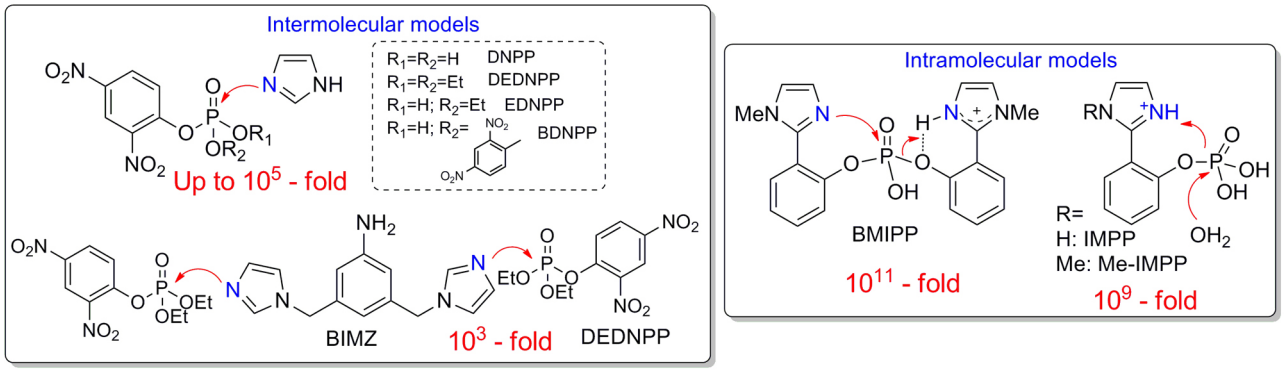

Scheme 1. IMZ-derived models and their catalytic efficiency.[7-11]

*e-mail: elisaorth@ufpr.br

nature of the reactions, accounting for the different forms of catalysis by IMZ. Thus, searching for a more realistic approach in modeling the notorious enzymatic characteristics such as hydrophobicity, approximation of the reactants and simultaneous multi-functionality of the reactive groups, catalytic polymers stands outs. Indeed, enzymes are biopolymers and engineering of macromolecules has great potential for designing artificial enzymes and gene delivery vectors.[12,13] Some studies are reported for acyl esters,[14-16] for example, molecularly imprinted polymers containing IMZ groups show 60-fold enhancements[17] and in another study a polymer containing carboxylate and IMZ group promoted 10^7-fold increments.[18] Recently, we proposed a polymeric nanoreactor with hydroxamate groups for phosphate ester cleavage that shows up to 10^6-fold enhancements,[19] although has the disadvantage of undergoing a "suicide attack",[20] i.e., is not an authentic recoverable catalyst. Polymers with IMZ and metal complexes have also been reported in the degradation of phosphotriester for the development of pesticide sensors.[21]

Moreover, micellar catalysis has also shown interesting enzymatic-like characteristics by promoting efficient approximation of reactants on the micellar domains by hydrophobic and/or electrostatic attraction.[22,23] Therefore, given the hydrophobic and potentially polyelectrolyte nature of polymers, micelles can easily potentiate these reactions.[19]

Herein, we studied the dephosphorylation reaction of the diester bis(2,4-dinitrophenyl) phosphate (BDNPP) and triester diethyl 2,4-dinitrophenyl phosphate (DEDNPP) with the catalytic polymer polyvinylimidazole (PVI) in the absence and presence of cationic (cetyltrimethylammonium bromide, CTABr) and anionic (sodium dodecyl sulfate, SDS) micelles, Scheme 2.

Experimental

Materials

PVI (Mw = 3500 g mol^{-1}), SDS and CTABr were obtained commercially and other reactants were of analytical grade. The phosphate esters BDNPP and DEDNPP were prepared by standard methods from $POCl_3$, as described previously.[7]

Potentiometric titrations

Titrations were carried out in a thermostated cell, under N_2 at 25.0 °C, at ionic strength 0.1 mol L^{-1} KCl, and [PVI] = 6.0 × 10^{-3} mol L^{-1}. The pH was monitored by a pHmeter upon addition of small increments of 0.1008 mol L^{-1} CO_2-free KOH using an automatic burette.

Kinetics

Reactions were followed spectrophotometrically by monitoring the appearance of 2,4-dinitrophenolate (DNP) at 400 nm. Reactions were carried out in 3 mL quartz cuvettes with a thermostated water-jacketed cell holder, by adding 10 µL of the substrate's stock solutions (10 × 10^{-3} mol L^{-1}, in acetonitrile) to aqueous solutions containing PVI under different conditions (concentration, temperature, pH). Observed first-order rate constants (k_{obs}) were calculated from data of absorbance *versus* time data for at least 90% of the reaction, using an iterative least-squares program; correlation coefficients were > 0.999 for all kinetic runs. The pH was self-buffered with PVI in the pH range of 6-8 and maintained with 0.01 mol L^{-1} buffers of $KHCO_3$ at pH 9-11.

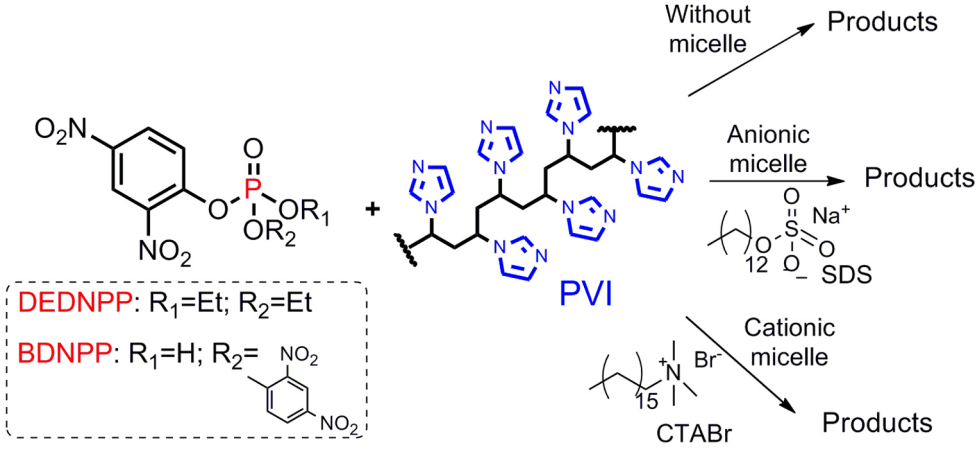

Scheme 2. Reactions studied herein.

Computational

Geometry optimization calculations were performed with the Gaussian 09 program[24] using the hybrid B3LYP combined with basis function 6-31+g(d). Subsequently, to obtain the final energy, single point calculations were performed with higher basis function 6-311+G(d,p) and same functional.

Results and Discussion

Potentiometric titration of PVI

As done in correlated studies,[19] it is important to evaluate the protonation equilibria of PVI to account for the reactive species and optimum pH conditions for the reaction. Therefore, potentiometric titration was carried out and the obtained curve is presented in Figure 1 along with data for IMZ for comparative purposes.[7] The titration results showed that PVI buffers in a wide range of pH (2-9), in contrast to IMZ that buffers between pH 6-8. It is known that an ionic species buffers at pH ± 1 of its pK_a, which agrees with the determined pK_a for IMZ (7.10). In the case of PVI, which has numerous IMZ ionic groups, multiple deprotonation equilibrium can occur, governed by several pK_a's, as illustrated in Figure 1. The deprotonation of a group must influence the neighboring group, so there may be several non-static pK_a's. Nevertheless, PVI shows an average pK_a around 5.8 (given by the derivative), well below the pK_a of the IMZ alone (7.1). The proposed equilibrium for the PVI is in agreement with the literature where authors report that IMZ groups have an average $pK_a = 6$ for *N*-vinylimidazole polymers.[25] Several studies show the equilibria complexity for poly(*N*-vinylimidazole),[26,27] for example, it was observed that the pH shift also leads to conformational changes in the polymer chain, which directly influences the protonation of the polymer. It was shown that the polymer contracts and then expands initially, during the stages of protonation, which is closely related to hydrogen bonding between the protonated and deprotonated IMZ rings.[28] Although complex, these dynamic equilibria can justify the catalytic reactivity of the polymer and possible artificial enzyme nature.

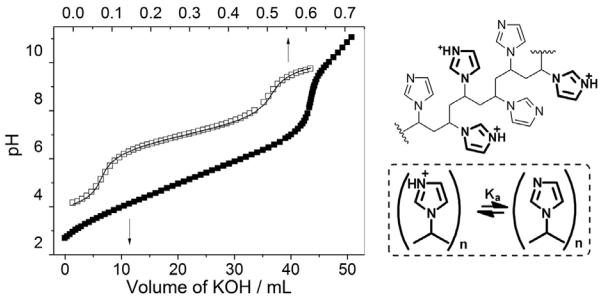

Figure 1. Potentiometric titration curves for PVI (6×10^{-3} mol L^{-1}, ■) and IMZ (1×10^{-3} mol L^{-1}, □) with KOH (0.1 mol L^{-1}) at 25 °C and equilibrium expected for PVI.

Kinetic study: without micelle

Kinetic studies were performed for the reactions of the diester BDNPP and triester DEDNPP with PVI, and pH profiles obtained are shown in Figure 2, along with respective spontaneous reactions.[7,29] Results show significant increases in k_{obs} for the dephosphorylation reactions in the presence of PVI: 1500-fold times and 50-fold for BDNPP and DEDNPP, respectively, compared with their spontaneous reactions at pH 8. In the reaction with DEDNPP, the profile reaches a non-varying k_{obs} region for pH > 7.5 indicating a nucleophilic pathway with reactive neutral IMZ groups. Curiously, with BDNPP, there is a subtle bell shaped profile, indicating that a bipolar specie with protonated and neutral IMZ groups is responsible for a bifunctional reaction, as observed in enzymes.[12] Figure 3 presents the pH profiles considering the local concentration of the IMZ moiety (k_{obs} / [monomer]), compared with the corresponding reactions with IMZ,[7] which shows for: (*i*) BDNPP, PVI is more reactive (ca. 5 times) than IMZ for pH < 8.5, but has similar reactivity at pH > 8.5; (*ii*) DEDNPP, IMZ is more reactive (ca. 7 times) than PVI in almost any pH range, except at pH < 5.5, where the reactivity are similar. Therefore, in the case of BDNPP, the cooperativity effect by the bipolar species is evidenced due to the higher reactivity of PVI in pH < 8.5, in contrast to IMZ, strongly indicating the contribution of a bifunctional catalysis by PVI. In the case of DEDNPP, the similar reactivity of PVI and IMZ is interesting since the one would expect the simple and small IMZ molecule to be more effective than the highly complex PIV polymeric architecture. Hence, the goal of reproducing the high efficiency of small IMZ-derived models in macromolecules was successfully accomplished herein, which is not always possible.[14] A related study with IMZ-derived polymer containing carboxylate groups was evaluated in the reaction of DEDNPP and showed lower k_{obs} values, but comparable second-order constants (considering the polymer concentration),[18] with the difference that herein the polymer is entirely functionalized with IMZ groups and we observed the characteristic bell-shaped pH profile.

Data in Figure 2 were fitted using equation 1 according to Scheme 3, that simplifies the complex reactions that can occur with PVI in two main paths, reaction with: (*i*) bipolar species with neutral and protonated IMZ groups present in the polymeric chain (k_{N1}), considered generically as PVI^+ and (*ii*) neutral IMZ groups (k_{N2}). This approach, although

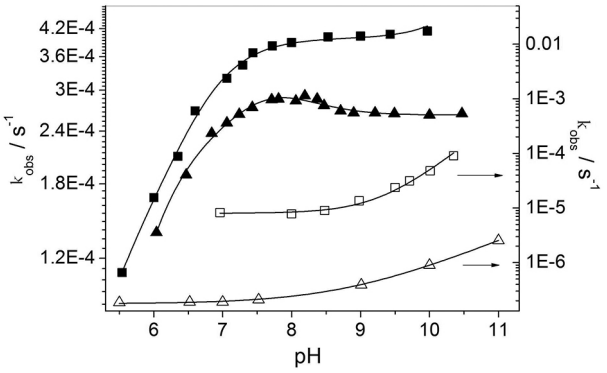

Figure 2. pH kinetic profile for the reaction of PVI (6×10^{-3} mol L^{-1}) with BDNPP (▲) and DEDNPP (■) at 25 °C. Corresponding spontaneous reaction is shown for comparison (△ and □, respectively).[7,29]

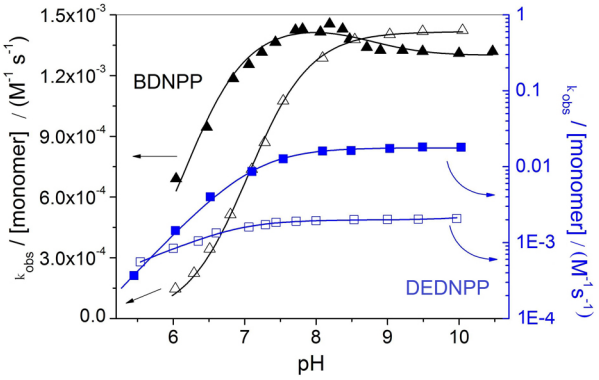

Figure 3. pH kinetic profile for the reaction of PVI, considering the monomer concentration (0.156 mol L^{-1}) with BDNPP (▲) and DEDNPP (■) at 25 °C. Respective reactions with IMZ (1 mol L^{-1}) is shown for comparison (△ and □, respectively).[7]

very simplistic, described well the k_{obs} increments as a function of pH, given the good correlation of the data with the theoretical fitting. The calculated kinetic parameters are shown in Table 1, and the second order constant of k_{N1} and k_{N2} are shown as a function of the total concentration of polymer and the monomer (k_{N1}^{m}, k_{N2}^{m}).

Table 1. Kinetic parameters obtained for the reactions with PVI[a]

	BDNPP	DEDNPP
k_0 / s^{-1}	1.90×10^{-7}	8.0×10^{-6}
k_{OH} / (M^{-1} s^{-1})	2.90×10^{-3}	3.40×10^{-1}
k_{N1} / (M^{-1} s^{-1}), [polymer][b]	3.60×10^{-2}	5.00×10^{-2}
k_{N1}^{m} / (M^{-1} s^{-1}), [monomer][c]	1.39×10^{-3}	1.92×10^{-3}
k_{N2} / (M^{-1} s^{-1}), [polymer][b]	2.90×10^{-2}	5.20×10^{-2}
k_{N2}^{m} / (M^{-1} s^{-1}), [monomer][c]	1.12×10^{-3}	2.00×10^{-3}

[a]Fiting curves in Figure 2 according to equation 1, based on Scheme 3, with kinetic $pK_{a1} = 6.55$ and $pK_{a2} = 8.25$, k_0 and k_{OH} are according to the literature;[7,29] [b][polymer] = 6×10^{-3} mol L^{-1}; [c][monomer] = 0.156 mol L^{-1}.

$$k_{obs} = k_0 + k_{OH}[OH^-] + [PVI]_T \times (k_{N1}\chi_{PVI+} + k_{N2}\chi_{PVI}) \quad (1)$$

Analysis of Figures 2 and 3, along with the parameters in Table 1 shows: (*i*) for BDNPP, the most reactive species is bipolar (k_{N1}), consistent with the bell-shaped pH profile behavior (Figure 2) characteristic of bifunctional catalysis, nonexistent in the DEDNPP profile. For DEDNPP, values of k_{N1} and k_{N2} are similar, which indicates that formation of neutral IMZ drives the reaction and solely a nucleophilic reaction is expected (typical pH profile plateau); (*ii*) compared with the spontaneous reaction (k_0), k_{N1} and k_{N2} (as a function of [polymer]) are 10^7 and 10^5-fold higher for BDNPP and DEDNPP, respectively. Further, comparing with the second order constant of the monomer, k_{N1}^{m} and k_{N2}^{m} are 10^5 and 10^4-fold for BDNPP

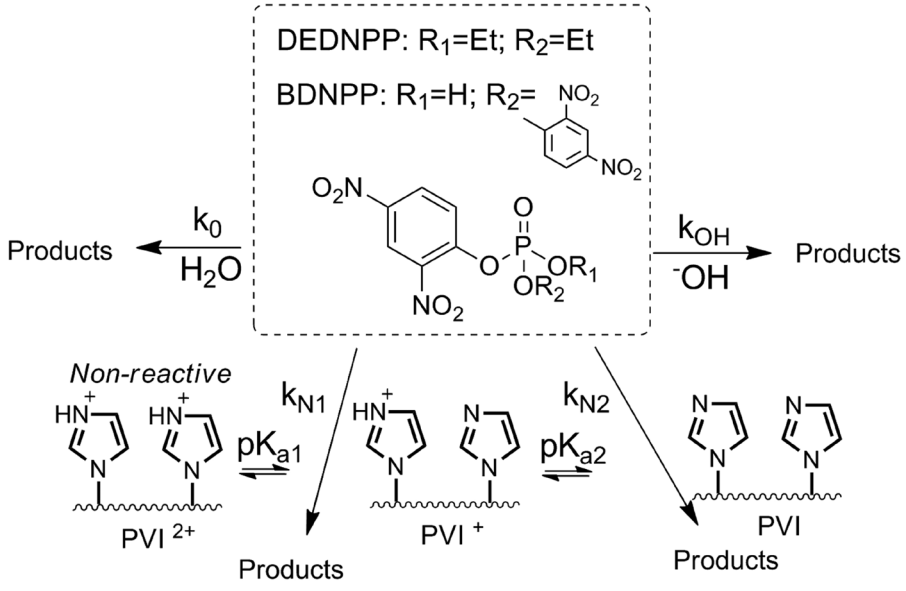

Scheme 3. Proposed reaction pathways for the reactions with PVI.

and DEDNPP, respectively. Increments for the reactions with IMZ for both esters are ca.10^3-fold,[7] indicating that the PVI has a prominent reactivity, especially in the reaction with BDNPP; (*iii*) the kinetic pK_{a1} agrees with titration data, although pK_{a2}, seems high, indicating that below this value there may be some sites where protonated IMZ are found and above this pH, all IMZ moieties are neutral, consistent the broad buffering capacity range of PVI. This effect can also be related to the complex nature of the PVI, which may undergo conformational change in the presence of a neutral (DEDNPP) or anionic ester (BDNPP), influencing directly in their protonation sites.

We propose that the dephosphorylation reaction with PVI occurs as depicted in Scheme 4 where a nucleophilic catalysis by neutral IMZ on the phosphorus atom, can or not be assisted by general-acid catalysis by a neighboring protonated IMZ group, activating the leaving group. Based on intra- and intermolecular designs detailed above with the IMZ group, in the reaction of BDNPP with PVI nucleophilic and general-acid catalysis should occur simultaneously, i.e., bifunctional, since the polymer can have regions with bipolar and/or neutral species. The protonated IMZ can also activate the ester via hydrogen bond with the P = O oxygen, as recently reported for ionically tagged (imidazolium-based) water-soluble artificial enzymes in dephosphorylation reactions.[30] This path would assist the nucleophilic attack by neutral IMZ and also lead to the bell-shaped pH profile. The general basic catalysis has not been considered important in the mechanism, whereas the catalytic increments are typical of nucleophilic reactions.[7] In the case of the reaction of DEDNPP with PVI, nucleophilic catalysis should dominate, leading to a phosphorylated intermediate, which decomposes, regenerating PVI and thus confirming an authentic catalytic cycle, as observed in other studies with IMZ.[7] The higher catalytic reactivity for the reaction with BDNPP can be related to the more hydrophobic structure of the ester, which may be more attracted to the hydrophobic polymer backbone.[16] In addition, the negative charge of BDNPP, combines effect of electrostatic approach by the positive charge of the polymer's protonated groups. Thus, PVI has micelle-like properties, e.g., incorporates (concentrates) reagents on its polymeric domain, and furthermore, exert catalytic functional role. This curious incorporation behavior is known for functional polyelectrolyte,[31-33] such as PVI, which combines multiple aspects of enzymatic catalysis: hydrophobic and electrostatic approach, and multi-functionality. In fact, the use of polymers as catalysts in dephosphorylation reactions is still little explored, and this work clarifies the potential of PVI as a possible artificial enzyme. Moreover, BDNPP is intrinsically less reactive than DEDNPP, hence is more feasible to a bifunctional catalysis. Previous study showed that less reactive esters undergo general base catalysis, in contrast to more activated esters that react via a nucleophilic pathway.[34] This can be extended to the present study in the sense that for BDNPP, an additional catalysis (general-acid) can benefit the reaction, while for DEDNPP a clear-cut nucleophilic attack rapidly cleaves the ester.

Kinetic study: with micelles

The reaction of PVI with DEDNPP and BDNPP was studied in the presence of cationic (CTABr) and anionic (SDS) micelle and pH profiles obtained are shown in Figure 4. It should be noted that the pH range studied in the

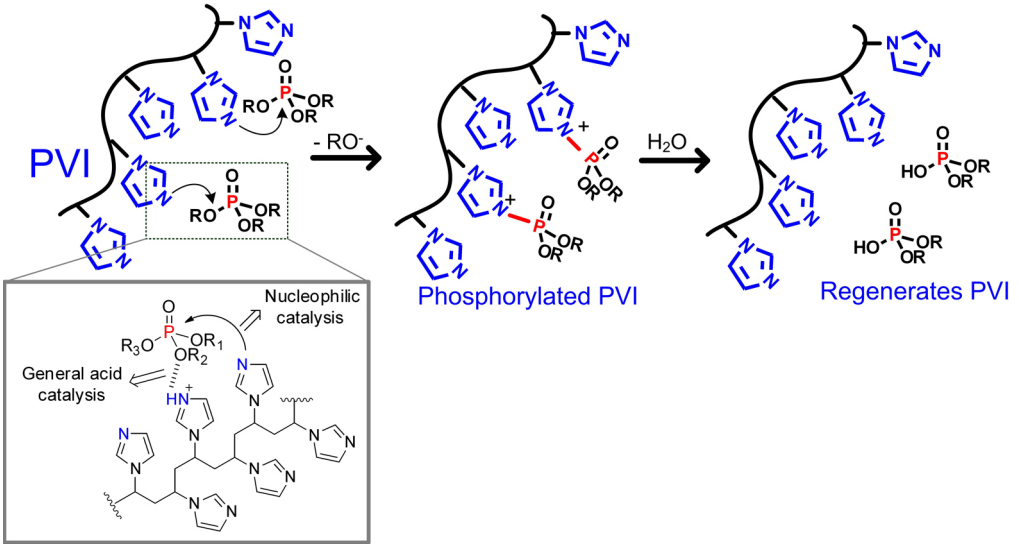

Scheme 4. Possible catalytic paths proposed for the reactions with PVI.

presence of micelles was limited by precipitation factors. In the case of the anionic diester BDNPP, the presence of CTABr inhibits up to 13-fold for pH < 8.5, but with SDS accelerates, although subtly 2-fold compared with its reaction with only PVI. The same reaction in the presence of CTABr for pH > 8.5 has k_{obs} values near those observed for the reaction in the absence of micelles. In the reaction with the neutral triester DEDNPP, we observe a peculiar micellar catalysis. In the presence of CTABr, for pH > 7.5, there was an increase in k_{obs} of up to 3-fold and with SDS, these increases reach 14-fold compared the reaction with solely PVI. The increments herein are typical of micellar catalysis,[15,16] but unusual because in the case of DEDNPP, there is an efficient catalysis by both cationic and anionic micelle, configuring a more versatile system. Normally, for reactions where cationic micelle accelerates, anionic micelle inhibits the reaction.[22]

Herein, cationic micelle CTABr strongly inhibits reactions at lower pH, probably due to the protonation of the reactive IMZ groups, which will be electrostatically repelled. Upon formation of neutral IMZ in the polymer chain, CTABr act more efficiently due to hydrophobic attraction, but micellar catalysis is only observed with DEDNPP. This can be explained by the bifunctional catalysis contribution (with the bipolar species), significant in the case of BDNPP. Although, BDNPP is negative and can be attracted by the cationic micelle, its inefficient catalysis evidences the significant contribution of the concomitant nucleophilic-general-acid catalysis (positively charged species). For DEDNPP, the reaction of the PVI is predominantly governed by the reactive neutral IMZ species, therefore, can be significantly catalyzed by CTABr due to hydrophobic attractions of the reactants. Interestingly, for BDNPP, SDS promotes micellar catalysis in the reaction with PVI, which should attract polymeric regions dominated by the bipolar species, but the expected repulsion of negatively charged BDNPP by SDS is not enough to inhibit the reaction, compared to only PVI. In the reaction with DEDNPP, SDS promotes more efficient micellar catalysis, as expected, due to the hydrophobic attraction of neutral reagents.

Overall, Figure 5 represents the interaction proposed for the efficient approximation of the reactants for reactions studied here. The hydrophobic micelle should approach the polymer and phosphate ester to its vicinity (hydrophobic forces and/or electrostatic), favoring dephosphorylation by IMZ groups of the polymer chain. Results evidence that hydrophobic attraction is the main driving force in the reactions with PVI, since no significant repelling of negative BDNPP by anionic SDS nor attraction by cationic CTABr is observed. Indeed, PVI and the esters are knowingly hydrophobic. Furthermore, theoretical modeling to describe the pH profiles of PVI reactions with the micelles is complex and requires further studies, which involve advanced techniques to evaluate the nature of polymer-micelle aggregates. Several studies have been published,[35,36] that focus only on detailing the interactions between micelles and polymers, using techniques such as surface tension, conductivity, fluorescence, microcalorimetry, and especially light scattering X-ray.[37] Authors propose up to three-dimensional phase diagram for these types of systems.[38] These more detailed studies have not been performed herein since the objective was only to expand knowledge regarding intermolecular reactions with IMZ-based catalysts for more complex, polymeric and micellar systems, and thus validate the efficiency of IMZ groups in macromolecular scaffolds and the reactant approximation in dephosphorylation reactions.

Computational study

Conformation analysis of the PVI was performed aiming to obtain information on its molecular structure and correlate with its reactivity. A pentamer of PVI was taken to represent the whole structure of the polymer and the presence of water as a solvent was simulated implicitly by

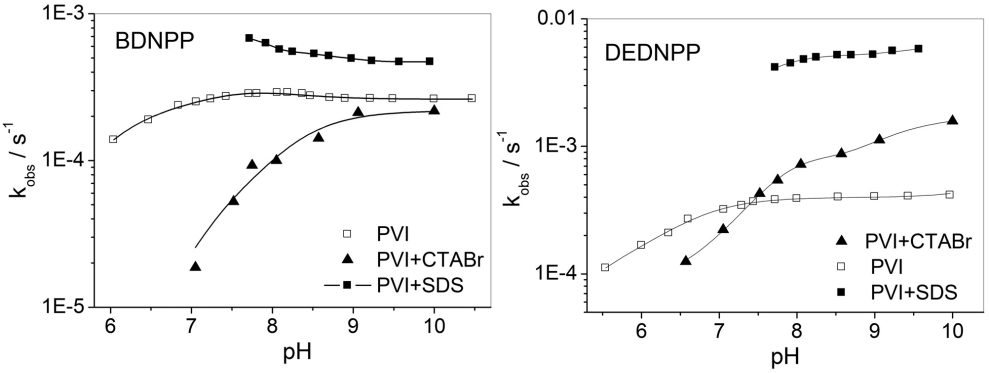

Figure 4. pH kinetic profile for the reaction of PVI (6×10^{-3} mol L^{-1}) in the presence of CTABr (0.01 mol L^{-1}) (-▲-) and SDS (0.01 mol L^{-1}) (-■-) with BDNPP and DEDNPP, 25 °C. The respective reactions in the absence of micelles is also shown (-□-).

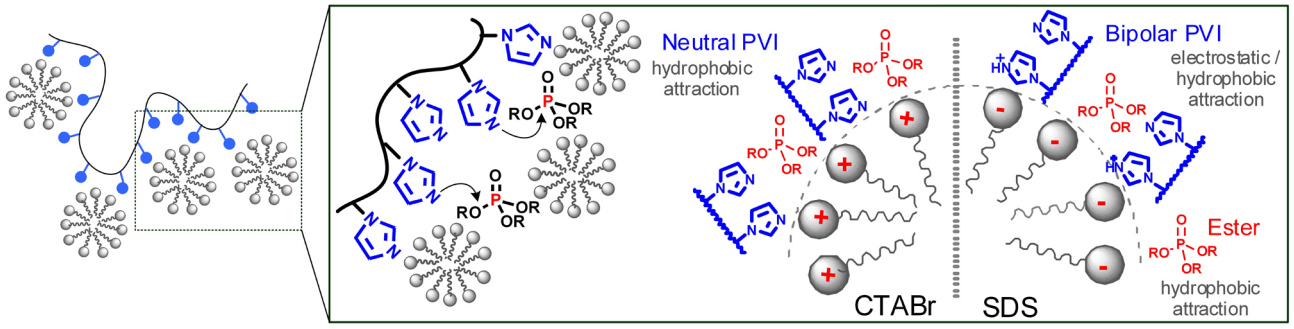

Figure 5. Representation of the dephosphorylation reactions with PVI in the presence of micelles.

polarizable continuum model (PCM) model with universal force field (UFF) radii. Initially, the conformation study was carried out based on syndiotactic (A_{sg}, B_{sg}) and isotactic (C_{sg}) polymer structures as starting geometries (sg) relative to the position of IMZ rings. In addition, two possibilities of syndiotactic geometries were proposed: with non-eclipsed (A_{sg}) and eclipsed (B_{sg}) nitrogen atoms along the carbon chain, as shown in Scheme 5.

Results show that the lowest energy conformation is that arising from the syndiotactic starting geometry (A_{opt}) since is 7.95 kcal mol^{-1} more stable than that optimized isotactic structure, wherein the rings are eclipsed along the chain. Further, between the two syndiotactic conformers, the structure with eclipsed IMZ rings (B_{opt}) shows energy 1.6 kcal mol^{-1} higher than conformer A_{opt}, as expected. The optimized structures are shown in Figure 6 and the results summarized in Table 2.

Based on the most stable structure of the PVI pentamer, corresponding to syndiotactic conformation with nitrogen atoms not eclipsed (A_{opt}), seven structures containing simple or double protonations were proposed in order to inquire the influence of the proton on the conformation of the chain. The interatomic distances of the nitrogen

Table 2. Relative free energies ΔG_{rel} of the PVI pentamers obtained with B3LYP/6-311+G(d,p)

	ΔG_{rel} / (kcal mol^{-1})
A_{opt}	0.0
B_{opt}	1.60954
C_{opt}	7.95544

atoms in the structures of protonated PVI are displayed in Table 3 (as labeled in Figure 6). Data related to the totally deprotonated geometry is shown for comparison proposes. In addition, in Figure 7 are shown the optimized structures A-H(3) e A-H(2)H(3), in which the number in brackets indicates the protonated ring (other structures are shown in the Supplementary Information section). Geometry parameters indicate in general that the inclusion of protons in the pentamer causes two electrostatic interactions between nearby pair of rings: (*i*) repulsive if rings are both protonated and (*ii*) attractive if one is protonated. More specifically, it is possible to observe in Table 3, for example, that the protonation of the ring 1 (structure A-H(1)) decreases its distance from 5.86899 to 4.38676 Å relative to the ring 3. On the other hand in structure A-H(1)H(3) the

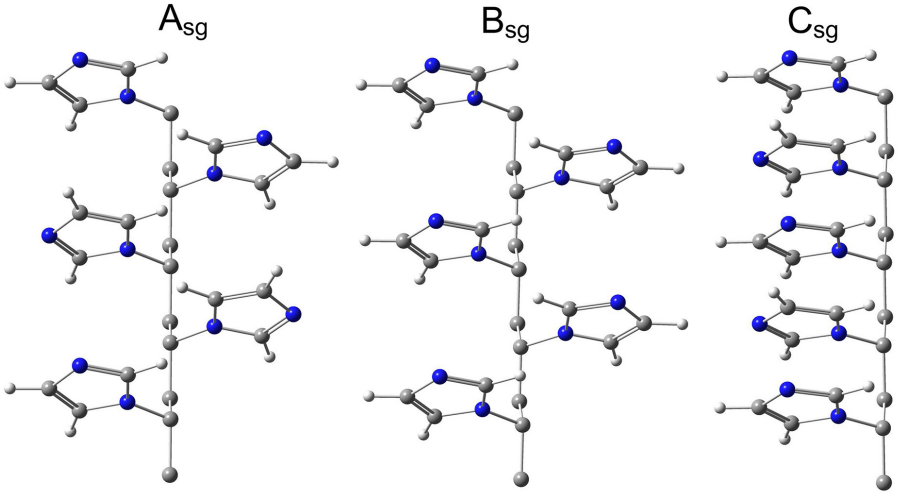

Scheme 5. Starting geometries (sg) for the conformational study of the PVI pentamer. A_{sg}: syndiotactic with non-eclipsed nitrogen atoms (blue balls), B_{sg}: syndiotactic with eclipsed nitrogen atoms and C_{sg}: isotactic.

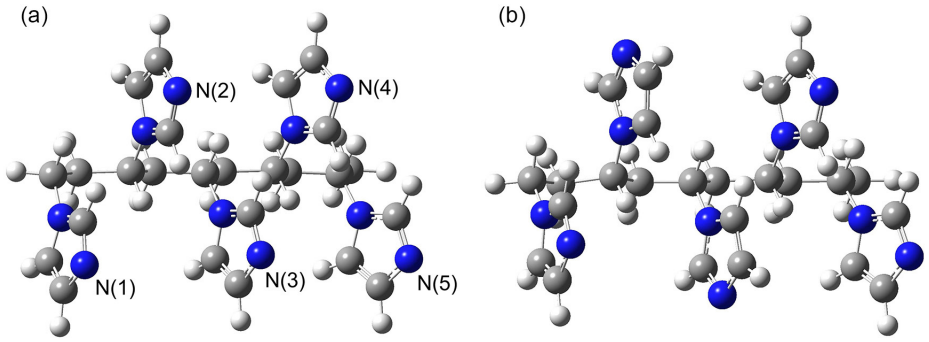

Figure 6. Optimized structures of PVI pentamer calculated from syndiotactic starting geometries with B3LYP/6-31+g(d). B_{opt} in (a) and A_{opt} in (b). The blue color indicates nitrogen, grey carbon and white hydrogen. The numbers in brackets indicate the label of the rings.

protonation of rings 1 and 3 leads its distance to 7.68823 Å indicating repulsion, but in the same time it generates an attractive interaction between rings 3 and 5, lowering the distance from each other to less than 4 Å. Interestingly, the protonation of ring 3 in A-H(3) yields to the approaching of rings 1 and 5, indicating that the molecule attempts to minimize the positive charge by changing its conformation. It is reasonable to inquire that the protonation of the PVI leads to an entanglement of the polymer, while the totally deprotonated structure must present a straight chain, based on similar distances between the rings IMZ (Table 3, A_{opt}).

These results can be correlated to the kinetic studies in the sense that the presence of bipolar species causes changes in the polymer conformation, effectively creating active sites, which can promote bifunctional catalysis for the reaction with BDNPP. These changes can also account for the possible attraction (electrostatic) between the negatively charged BDNPP and bipolar site PVI^{+}. For DEDNPP, this attraction is not possible (neutral ester) and the polymer is preferentially linear, as shown in other nucleophilic polymers.[18]

Conclusions

The results presented for the dephosphorylation reactions in the presence of the IMZ-derived polymeric catalyst PVI, confirms the catalytic potential of IMZ groups anchored on the macromolecular chain, with increments up to 10^7-fold. Two phosphate esters were studied, which seem to follow different mechanistic pathways. For the triester, a nucleophilic catalysis is proposed and for the diester, results indicate a bifunctional nucleophilic-general-acid catalysis, with a protonated IMZ assisting the leaving group, while a neutral IMZ attacks the phosphorus atom. Computational studies were done to corroborate the conformation of the polymer, indicating significant changes for the bipolar and neutral species, accounting for distinct regions on the polymer, like active sites. Whereby, PVI is multifunctional since it can attract the reactants on its domain (hydrophobic/electrostatic forces) and effectively catalyze the ester's cleavage. Hence, PVI acts as an artificial enzyme, because it has enzymatic attributes with active sites, hydrophobic nature and important conformational and proximity contributions in reactivity. In addition, the micellar catalysis proved to be important in the reactions studied, since facilitates a more efficient approach of the reactants and also confirms the reactivity of the bipolar species. Studies with functional polymers have attracted great interest since they have different applications,[19,20] for example, to obtain nanocomposites with special properties for electrochemical sensors and bioactive synthetic polymers, which have intrinsic therapeutic properties in recognition and removal of unwanted substances in the gastrointestinal tract.[39]

Table 3. Distances between IMZ rings of PVI pentamer, based on nitrogen atoms as labeled in Figure 6. The numbers in brackets indicate the label of the rings

Distance of rings / Å	A_{opt}	A-H(1)	A-H(3)	A-H(1)H(3)	A-H(1)H(4)	A-H(2)H(3)	A-H(2)H(4)
N(1)-N(2)	5.86077	5.11700	5.81512	4.77653	5.13278	5.24776	3.93417
N(1)-N(3)	5.86899	4.38676	4.94754	7.68823	6.30444	5.36805	5.86688
N(2)-N(3)	5.61677	6.10230	5.08714	5.90002	5.62942	7.14578	5.29933
N(2)-N(4)	5.89655	5.91453	5.53589	5.70136	6.22177	3.32652	7.25825
N(3)-N(4)	5.68495	5.42596	4.84927	5.03311	5.57697	6.54686	5.46683
N(3)-N(5)	5.83428	5.97881	4.99266	3.96537	5.96934	3.17903	5.89756
N(4)-N(5)	5.75327	5.81882	5.78089	6.10586	3.97400	6.42284	3.91058

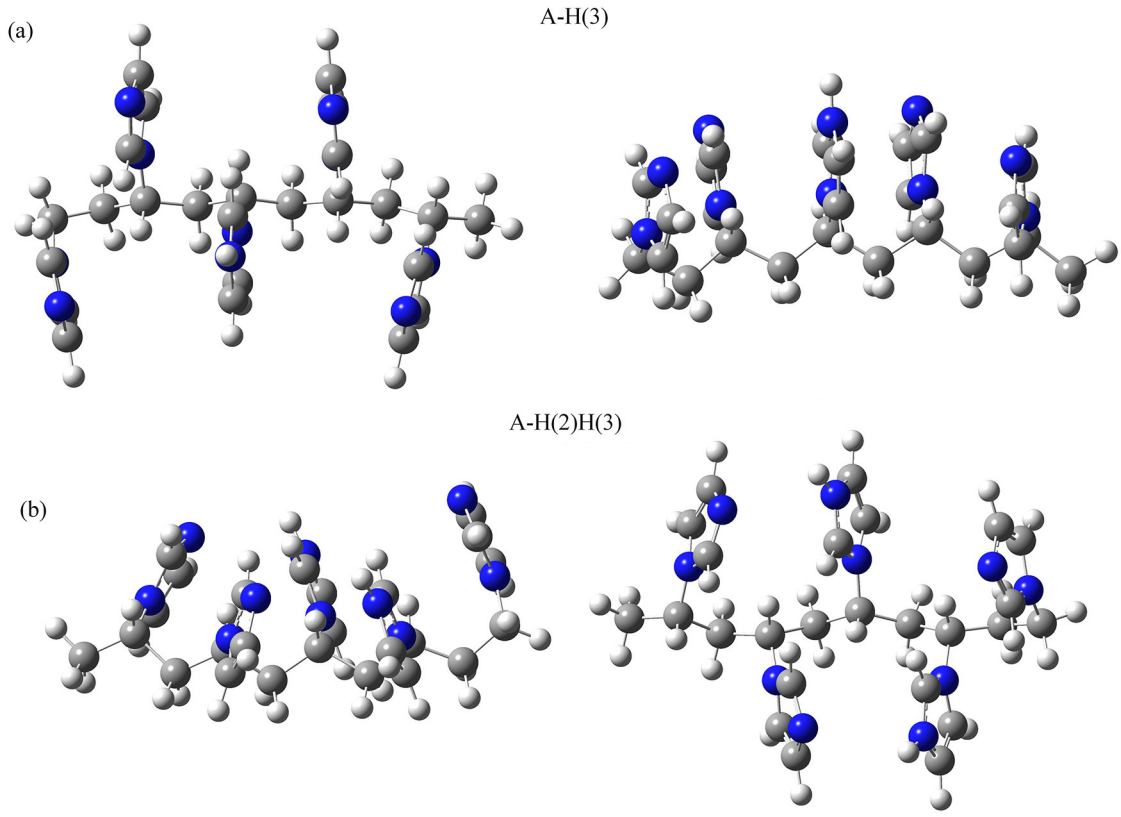

Figure 7. Optimized structures of syndiotactic PVI pentamer with single (A-H(3)) in (a) and double (A-H(2)H(3)) protonation using B3LYP/6-31+g(d) in (b).

In this context, polymers with IMZ and/or imidazolium groups (salts, ionic liquids, etc.) have shown great therapeutic importance because they can provide antimicrobial, antiarrhythmic and anti-metastatic activity. Likewise, the design of IMZ-derived polymers for therapeutic purposes is still relatively recent.[2] Yet, this type of polymer has also shown characteristics of stimuli response materials. Although this work has not addressed aspects of biological activity and applications, the results are important because they show that the PVI reacts efficiently with phosphate esters. These are abundant in biological systems, not only in DNA chain but also in the form of phosphorylated enzyme intermediates and other species (ATP, ADP), determinants in several biological functions such as signaling processes. Finally, this study has potential for detoxification purposes, since many toxic chemicals (chemical warefare, pesticides) are phosphate esters, which require adequate disposal and elimination of their toxicity,[40] i.e., by an efficient multifuctional catalytic system, such as proposed herein.

Supplementary Information

Supplementary Information (calculation data of optimized geometries) is available free of charge at http://jbcs.sbq.org.br.

Acknowledgements

Authors acknowledge the financial support from CNPq, CAPES, Fundação Araucária, INCT-Catalysis, UFPR, UTFPR and UFSC.

References

1. Westheimer, F. H.; *ACS Symp. Ser.* **1992**, *486*, 1.
2. Anderson, E. B.; Long, T. E.; *Polymer* **2010**, *51*, 2447.
3. Attwood, P. V.; Piggott, M. J.; Zu, X. L.; Besant, P. G.; *Amino Acids* **2007**, *32*, 145.
4. Puttick, J.; Baker, E. N.; Delbaere, L. T. J.; *Biochim. Biophys. Acta, Proteins Proteomics* **2008**, *1784*, 100.
5. Klumpp, S.; Krieglstein, J.; *Eur. J. Biochem.* **2002**, *269*, 1067.
6. Raines, R. T.; *Chem. Rev.* **1998**, *98*, 1045.
7. Orth, E. S.; Wanderlind, E. H.; Medeiros, M.; Oliveira, P. S. M.; Vaz, B. G.; Eberlin, M. N.; Kirby, A. J.; Nome, F.; *J. Org. Chem.* **2011**, *76*, 8003.
8. Brandão, T. A. S.; Orth, E. S.; Rocha, W. R.; Bortoluzzi, A. J.; Bunton, C. A.; Nome, F.; *J. Org. Chem.* **2007**, *72*, 3800.
9. Orth, E. S.; Brandao, T. A. S.; Milagre, H. M. S.; Eberlin, M. N.; Nome, F.; *J. Am. Chem. Soc.* **2008**, *130*, 2436.
10. Orth, E. S.; Brandao, T. A. S.; Souza, B. S.; Pliego, J. R.; Vaz,

B. G.; Eberlin, M. N.; Kirby, A. J.; Nome, F.; *J. Am. Chem. Soc.* **2010**, *132*, 8513.

11. Wanderlind, E. H.; Orth, E. S.; Medeiros, M.; Santos, D. M. P. O.; Westphal, E.; Gallardo, H.; Fiedler, H. D.; Nome, F.; *J. Braz. Chem. Soc.* **2014**, *12*, 2385.
12. Breslow, R.; *Artificial Enzymes*; Wiley-VCH: Weinheim, 2005.
13. Midoux, P.; Pichon, C.; Yaouanc, J. J.; Jaffres, P. A.; *Brit. J. Pharmacol.* **2009**, *157*, 166.
14. Kitano, H.; Sun, Z. H.; Ise, N.; *Macromolecules* **1983**, *16*, 1306.
15. Kunitake, T.; Shinkai, S.; *J. Am. Chem. Soc.* **1971**, *93*, 4256.
16. Overberger, C. G.; Mitra, S.; *Abstr. Pap., Jt. Conf. - Chem. Inst. Can. Am. Chem. Soc.* **1978**, *175*, 57.
17. Chen, W.; Han, D. K.; Ahn, K. D.; Kim, J. M.; *Macromol. Res.* **2002**, *10*, 122.
18. Giusti, L. A.; Medeiros, M.; Ferreira, N. L.; Mora, J. R.; Fiedler, H. D.; *J. Phys. Org. Chem.* **2014**, *27*, 297.
19. Mello, R. S.; Orth, E. S.; Loh, W.; Fiedler, H. D.; Nome, F.; *Langmuir* **2011**, *27*, 15112.
20. Orth, E. S.; da Silva, P. L. F.; Mello, R. S.; Bunton, C. A.; Milagre, H. M. S.; Eberlin, M. N.; Fiedler, H. D.; Nome, F.; *J. Org. Chem.* **2009**, *74*, 5011.
21. Yamazaki, T.; Yilmaz, E.; Mosbach, K.; Sode, K.; *Anal. Chim. Acta* **2001**, *435*, 209.
22. Dwars, T.; Paetzold, E.; Oehme, G.; *Angew. Chem. Int. Edit.* **2005**, *44*, 7174.
23. Bunton, C. A.; *Arkivoc* **2011**, *vii*, 490.
24. Frisch, M. J.; Trucks, G. W.; Schlegel, H. B.; Scuseria, G. E.; Robb, M. A.; Cheeseman, J. R.; Scalmani, G.; Barone, V.; Mennucci, B.; Petersson, G. A.; Nakatsuji, H.; Caricato, M.; Li, X.; Hratchian, H. P.; Izmaylov, A. F.; Bloino, J.; Zheng, G.; Sonnenberg, J. L.; Hada, M.; Ehara, M.; Toyota, K.; Fukuda, R.; Hasegawa, J.; Ishida, M.; Nakajima, T.; Honda, Y.; Kitao, O.; Nakai, H.; Vreven, T.; Montgomery Jr., J. A.; Peralta, J. E.; Ogliaro, F.; Bearpark, M. J.; Heyd, J.; Brothers, E. N.; Kudin, K. N.; Staroverov, V. N.; Kobayashi, R.; Normand, J.; Raghavachari, K.; Rendell, A. P.; Burant, J. C.; Iyengar, S. S.; Tomasi, J.; Cossi, M.; Rega, N.; Millam, N. J.; Klene, M.; Knox, J. E.; Cross, J. B.; Bakken, V.; Adamo, C.; Jaramillo, J.; Gomperts, R.; Stratmann, R. E.; Yazyev, O.; Austin, A. J.; Cammi, R.; Pomelli, C.; Ochterski, J. W.; Martin, R. L.; Morokuma, K.; Zakrzewski, V. G.; Voth, G. A.; Salvador, P.; Dannenberg, J. J.; Dapprich, S.; Daniels, A. D.; Farkas, O.; Foresman, J. B.; Ortiz, J. V.; Cioslowski, J.; Fox, D. J.; *Gaussian 09*; Gaussian Inc., USA, 2009.
25. Asayama, S.; Hakamatani, T.; Kawakami, H.; *Bioconjugate Chem.* **2010**, *21*, 646.
26. Horta, A.; Molina, M. J.; Gomez-Anton, M. R.; Pierola, I. F.; *J. Phys. Chem. B* **2008**, *112*, 10123.
27. Masaki, M.; Ogawa, K.; Kokufuta, E.; *Colloid Polym. Sci.* **2009**, *287*, 1405.
28. Henrichs, P. M.; Whitlock, L. R.; Sochor, A. R.; Tan, J. S.; *Macromolecules* **1980**, *13*, 1375.
29. Bunton, C. A.; Farber, S. J.; *J. Org. Chem.* **1969**, *34*, 767.
30. Ferreira, J. G. L.; Ramos, L. M.; Oliveira, A. L.; Orth, E. S.; Neto, B. A. D.; *J. Org. Chem.* **2015**, *80*, 5979.
31. Manning, G. S.; *Acc. Chem. Res.* **1979**, *12*, 443.
32. Ghimici, L.; Dragan, S.; *Colloid Polym. Sci.* **2002**, *280*, 130.
33. Choucair, A.; Eisenberg, A.; *J. Am. Chem. Soc.* **2003**, *125*, 11993.
34. Neuvonen, H.; *J. Chem. Soc., Perkin Trans. 2* **1995**, 951.
35. Sorci, G. A.; Reed, W. F.; *Langmuir* **2002**, *18*, 353.
36. Hansson, P.; *J. Phys. Chem. B* **2009**, *113*, 12903.
37. Romani, A. P.; Gehlen, M. H.; Itri, R.; *Langmuir* **2005**, *21*, 127.
38. Svensson, A.; Piculell, L.; Cabane, B.; Ilekti, P.; *J. Phys. Chem. B* **2002**, *106*, 1013.
39. Dhal, P. K.; Polomoscanika, S. C.; Avilaa, L. Z.; Holmes-Farleya, S. R.; Miller, R. J.; *Adv. Drug Delivery Rev.* **2009**, *61*, 1121.
40. Orth, E. S.; Almeida, T. G.; Silva, V. B.; Oliveira, A. R. M.; Ocampos, F. M. M.; Barison, A.; *J. Mol. Catal. A: Chem.* **2015**, *403*, 93.

Submitted: July 17, 2015
Published online: Sptember 4, 2015